ELSEVIER

Biochemical Engineering Journal 37 (2007) 285–293

Biochemical Engineering Journal

www.elsevier.com/locate/bej

Modelling diffusivity in porous polymeric membranes with an intermediate layer containing microbial cells

Manuel Mota [a,*], Alexander Yelshin [a], Marcello Fidaleo [c], Michael C. Flickinger [b]

[a] *IBB – Institute of Biotechnology and Bioengineering, Centre for Biological Engineering, Universidade do Minho, Campus de Gualtar, 4710-057 Braga, Portugal*

[b] *Department of Biochemistry, Molecular Biology and Biophysics, University of Minnesota, St. Paul, MN 55108, USA*

[c] *Department of Food Science and Technology, University of Tuscia, 01100 Viterbo, Italy*

Received 24 January 2006; received in revised form 8 May 2007; accepted 18 May 2007

Abstract

Three-layer systems (membrane – composite layer (cells + polymer) – membrane) are important in different biochemical applications. Models of latex layered-membranes were evaluated and compared with experimental data in order to predict the diffusivity of substrates in the composite layer containing living *E.coli* microbial cells. Diffusivity predictions are dependent on the presence or the absence of a 'skin' layer, on the degree of polymer particle coalescence and on the thickness of each layer. Simulations with layered models were made to identify the dominant mechanisms in the three-layer system. It was found that the layered system is sensitive to the latex coatings porosity when the composite layer occupies less than 50% of the total membrane system thickness. Whenever the control of polymer particle coalescence and of the layers (coating/composite layer) thickness may be achieved, multi-layer systems presenting a wide range of relative diffusion conductivities may be built for different types of living cells and for a wide variety of practical applications. The diffusivity of the latex layer is proportional to the square of latex porosity.

Keywords: Diffusion; Microporous membrane; Immobilised cells; Modelling; Packing; Mass transfer

1. Introduction

Multi-layer microporous systems have a wide application in industry and biotechnology and their general models are described in numerous publications [1–9]. In the biotechnology layered systems have a broad application [10] including, in particular, systems containing living cells: thick-film and immobilized cell biosensors [11–14], components of bioelectronic devices [15–17], or biocatalytic coatings [18].

Among these systems we may distinguish porous layers and membranes, which are forming by polymer latex of sub-micron sizes [19,20]. Concerning the biocatalyst application, such systems have a structural diversity of membranes and composite (cell + latex) layers because of particle size distribution, shape, layers thickness, packing and formation conditions as well as technological demands [18,21–23]. The promising type of thin-membrane bioreactor consists of a high volume fraction of viable, metabolically active whole cells imprisoned in a porous polymeric matrix of partially coalesced latex particles that are substantially smaller than the bacterial cells.

A method for immobilising viable but non-growing *Escherichia coli* in highly uniform patches was considered by Lyngberg et al. [21]. The method allows the composite (cell + polymer) layer and the polymer sealant to be variable in thickness from 5 to 60 μm and from 7 to 80 μm, respectively.

The polymer latex coating micro-structure for whole-cell biocatalyst application was investigated by microscopy [22]. Results showed that porosity and permeability can be controlled by appropriate drying and rehydration protocols. Evidence shows that glycerol retards particle deformation, compaction, and coalescence. The microstructure of a biocatalytic latex coating containing viable *E. coli* cells was analysed in [23,24]. The cells are physically entrapped by the latex particles and not chemically bound to them and cells were uniformly distributed in the matrix.

Another multi-layer system, a permeable biocatalytic coating of thin layers of 280 nm particle size latex containing *E. coli* mixed with latex particles, was also investigated in the work of Lyngberg et al. [18]. The effective diffusion coefficient D_e of the system was measured and compared with those D_0 in bulk

* Corresponding author. Tel.: +351 25360 1191.
E-mail address: MMota@reitoria.uminho.pt (M. Mota).

1369-703X/$ – see front matter © 2007 Elsevier B.V. All rights reserved.
doi:10.1016/j.bej.2007.05.008

Nomenclature

D_0	diffusion coefficient in bulk liquid (m^2/s)
D_e	effective diffusion coefficient (m^2/s)
h	diameter of the rod (m)
K	overall mass transfer coefficient (m/s)
k	mass transfer coefficient of the multi-layer system (m/s)
k_{p1}, k_{p2}	respectively, mass transfer coefficients in phase 1 and 2 separated by the layered system (m/s)
k_i	mass transfer coefficient in i-th layer (m/s)
L	multi-layer system thickness (m)
L'	diffusion pathway (m)
l_i	thickness of i-th layer (m)
m	number of sub-layers in the composite layer
n	number of layers in the system
T	tortuosity
x_c	volume fraction of cells in the composite layer
y_i	linear fraction of i-th layer thickness in the total system thickness
ε_c^0	porosity of pure cell packing
ε_i	the i-th layer porosity
ε_{lx}^0	porosity of pure latex packing
δ	ratio of the cell length/diameter
ϕ_c	cell volume concentration in the composite layer
$\eta = D_e/D_0$	system relative diffusion conductivity
τ	tortuosity factor
τ_i	tortuosity factor of i-th layer

Indexes

c	cell fraction
clx	composite layer (cells + latex)
i	characteristics of i-th layer
j	characteristics of j-th sub-layer in the composite layer
f	polymer film characteristics
lx	latex layer in the form of the spherical particles packing
lx + s	latex layer with skin
lx + clx + s	three-layer system with skin on the border of one of the latex coating
s	skin (layer) of the flattened latex particles
sp	skin with distributed within pore space dispersed phase or polymer film

fluid. It was found that a ratio $\eta = D_{lx}/D_0$ of latex coatings varies from 3×10^{-4} for unmodified latex coating to 6.8×10^{-2} for coatings containing sucrose, where D_{lx} is the effective diffusion coefficient in the latex layer. The results were explained by postulating a flattening of the latex particles against the surface of the solid substrate on which the coating was cast, as well as by the presence of a colloid stabiliser. Latex coatings were cast on stainless steel and delaminated to build three-layer composites containing viable *E. coli* mixed with latex particles in the middle layer.

The term diffusivity is generally used with the same meaning as diffusion coefficient (see: "Chemical diffusion coefficient, Fick's first law, partial diffusion coefficient" [80]) and will be used in this work meaning a "capacity to allow diffusion" [81]. Several effects acting on the diffusivity of layered systems can be identified: micro-structure of the composite layer is dependent on the packing structure, on density as well as on a particle (cell/latex) size ratio, thickness, structural characteristics of the coatings, among others [18,22]. A detailed overview of the layered systems to be considered in this work may be found in recently published papers [78,79].

2. Theoretical background

A multi-layered system may be characterised by a conventional mass transfer model [2,6,25,26]. A layered permeable system mass transfer coefficient K, in general, depends on the phase conditions and on the layered system properties; if the system is in-between phases, then $1/K = 1/k_{p1} + 1/k + 1/k_{p2}$, where k_{p1}, k_{p2} and k is, respectively, the mass transfer coefficients in phase 1, 2, and in the layered system. When the mass transfer resistance is concentrated at the permeable layers, then it is possible to assume that $1/K \cong 1/k$ and for diffusion through the layered system the above expression is simplified to

$$\frac{1}{k} = \sum_{i=1}^{n} \frac{1}{k_i} \tag{1}$$

where k is the n-th layer system mass transfer coefficient, k_i is the mass transfer coefficient of the i-th layer, and n is number of layers in the system.

If diffusion is not affected by a hindrance effect [27] and assuming also that, different layers have different porosity and tortuosity, then the mass transfer coefficient k_i is represented as

$$\frac{1}{k_i} = \frac{l_i \tau_i}{(D_0 \varepsilon_i)} \tag{2}$$

where D_0 is the diffusion coefficient of solute in bulk liquid and for the i-th layer, l_i is the layer thickness, τ_i is the tortuosity factor, and ε_i is the layer porosity.

The problem becomes more complex in the case of a non-homogeneous system with significant differences in porosity and tortuosity [26,28–32].

In the case of immobilised cells, depending on conditions, cells may be distributed non-homogeneously within the porous matrix. The non-homogeneous cell distribution may have the form of a confined cell sub-layer in a composite layer with an anisotropic cell concentration distribution [33,34]. Cells may be distributed, for instance, with a gradual concentration in the total volume of the porous medium. They may also be different in shape, spatial orientation, type of aggregation of the microbial population, etc. [35–44]. The immobilised cell system effective diffusivity is therefore, affected by two main components: polymer composition; cell presence and cellular spatial distribution [45,46].

In general, multi-layer systems may have either a capillary nature or a structure generated by monosize particle packing, by

particle mixtures of different sizes, and by particles distributed within a polymer or gel matrix [46,47]. Several types of possible arrangements in multi-layered systems (including sub-layers) are going to be considered in order to evaluate the best fit for the case of the latex three-layer systems described by Lyngberg et al. [18].

In the absence of a convective flow, the equation governing diffusion in micro porous media is the Fick diffusion law and diffusion may be characterised by an effective diffusion coefficient D_e [27,47]. The effective diffusion coefficient for the porous media D_e depends on D_0, on porosity, and on tortuosity: $D_e = D_0\varepsilon/\tau$. The ratio $\eta = D_e/D_0 = \varepsilon/\tau$ is a widely used parameter, defined as the relative diffusion conductivity of a porous medium. With the ratio η the system mass transfer coefficient can be written as

$$k = \frac{D_e}{L} = \frac{D_0\varepsilon}{\tau L} = \frac{D_0\eta}{L} \tag{3}$$

where L is the total layered system thickness, whereas ε and τ represent the system equivalent porosity and tortuosity.Based on relations (2) and (3) Eq. (1) becomes

$$L/\eta = \sum\nolimits_{i=1}^{n} l_i/\eta_i \tag{4}$$

and after normalisation

$$\frac{1}{\eta} = \sum_{i=1}^{n} \frac{y_i}{\eta_i} \tag{4a}$$

or

$$\eta = \frac{1}{\sum_{i=1}^{n} y_i/\eta_i} \tag{4b}$$

where $y_i = l_i/L$ is the linear fraction of i-th layer thickness in the total system thickness, L, $\sum y_i = 1$.

The model (4) elicits the simulation of a layered system response of η to the spatial variation of ε_i, τ_i, y_i, and n in the diffusional process. Furthermore, different scenarios such as particle overlapping, flattening, presence of colloid stabiliser, and matrix/cells size ratio may be tested.

3. Multi-layer system model

In ideal conditions the model (4b) transforms to a three-layer system, and

$$\eta = \frac{1}{(y_{(lx)1}/\eta_{(lx)1} + y_{clx}/\eta_{clx} + y_{(lx)2}/\eta_{(lx)2})} \tag{5}$$

where $\eta_{(lx)1}$, $\eta_{(lx)2}$ are, respectively, the relative diffusion conductivity of coatings on both size of the composite layer and η_{clx} is the relative diffusion conductivity of composite layer (latex + cells). Assuming that the coating properties are similar, then $\eta_{lx} = \eta_{(lx)1} = \eta_{(lx)2}$.

3.1. Composite layer

For composite layers (latex particles + cells) the tortuosity of the porous medium is defined by the pore topology and is a product of the composition content [47–51]. If cells are assumed to be impermeable, the composite relative diffusion conductivity η_{clx} is the product of the relative diffusion conductivity of the polymer (latex) matrix, $\eta_{lx} = D_{lx}/D_0$, with relative diffusion conductivity created by the presence of cells, $\eta_c = D_{clx}/D_{lx}$, which leads to the expression

$$\eta_{clx} = \frac{D_{clx}}{D_0} = \eta_{lx}\eta_c \tag{6}$$

In the case of a non-homogeneous cell distribution within the composite layer, model (6) becomes complex but in some specific conditions the model can be presented as the combination of (4b) and (6). The gradually decreasing cell concentration from the top of the matrix surface to the inner side may be represented by a stepped sub-layer system where in each layer the cell concentration is assumed to be constant [47]. In this approach, the application of Eq. (4b) to the composite layer diffusion conductivity gives

$$\eta_{clx} = \frac{1}{\sum_{j=1}^{m} y_j/\eta_{(clx)j}} \tag{7}$$

where $j = 1, \ldots, m$ is the number of sub-layers in the composite layer and $\eta_{(clx)j}$ is the diffusion conductivity of j-th sub-layer defined by Eq. (6): $\eta_{(clx)j} = \eta_{(lx)j}\eta_{(c)j}$. When one of the components (matrix or cells) is distributed homogeneously in the composite, model (7) simplifies: $\eta_{(lx)j}$ or $\eta_{(c)j}$ becomes constant.

3.2. Coating layers

Latex may be considered as made of spherical particles, which according to Shimizu et al. [52], behave like spheres in the absence of additional effects [23]. A homogeneous latex layer may thus be considered as a uniform packing, formed by monosized particles, which means that the following equation may be applied

$$\eta_{lx} = \frac{\varepsilon_{lx}}{\tau_{lx}} \tag{8}$$

where η_{lx} is the latex layer relative diffusion conductivity, ε_{lx} and τ_{lx} are the porosity and tortuosity factor of the latex layer, respectively.

Latex particles may be affected by film formation and coat drying as may be analysed in the following lines.

3.2.1. Latex layer with flattened polymer particle—"skin"

Micrographs of the latex layer proved the existence of a flattened latex particle "skin" layer in contact with the flat stainless steel substrate used for film casting [18]. The measurements showed that the flattened layer thickness matched the latex particle size, Fig. 1.

Relative diffusion conductivity of the latex layer with a flattened skin, $\eta_{(lx+s)}$, can be represented as a bi-layer model based on (4b):

$$\eta_{(lx+s)} = \frac{1}{[y_{lx}/\eta_{lx} + (1 - y_{lx})/\eta_s]} \tag{9}$$

where $y_{lx} = l_{lx}/(l_{lx} + l_s)$ is the thickness fraction of the latex layer with properties of spherical particle bed, and η_s is the

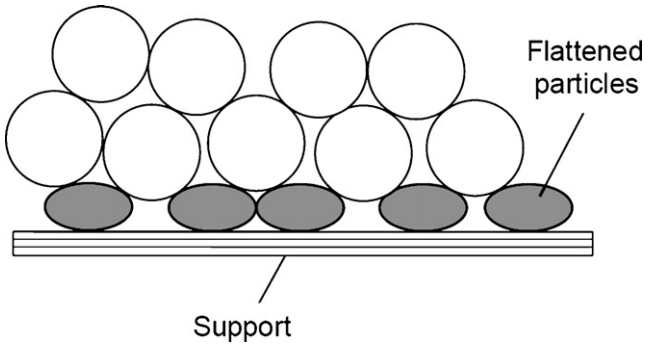

Fig. 1. The flattened latex particle layer (grey) on the flat support with blocked pores caused by non-flattened latex particles (white).

relative diffusion conductivity of the skin formed by flattened particles.

To extend the model framework, let us consider now a case when a nano-particles or polymer in the form of film are present in pores of the latex skin. The relative diffusion conductivity of the skin with homogeneous nano-particles or polymer film distribution in the pores, η_{sp}, may be represented in the form [50,51]

$$\eta_{sp} = \eta_s \eta_p \tag{10}$$

where η_p is the relative diffusion conductivity of nano-particles packing or polymer film in the skin pores.

Finally, based on Eq. (7) and taking into account relations (8)–(10) we can analyse layered system in details.

4. Modelling and discussion

For understanding the influence of different factors on the system permeability, factors are dividing on two groups: factors acting in coatings and factors important for composite layer. Below, we consider at first each of groups and than analyse all system coatings + composite layer.

4.1. Coating layers

One of the methods used to obtain the latex film for the coating is based on a mixture of latex with glycerol, to prevent latex particles from coalescing or compacting (overlapping) during film formation. Measurements of the relative diffusion conductivity η_{lx} for latex coatings gave values ranging from $\eta_{lx} = 0.003$ (without glycerol) up to 0.057 (with 0.15 volume units of glycerol/volume unit of dry polymer) [18,22]. Moreover, for very thin layers of the latex particle size, the relative diffusion conductivity reduced up to 0.0003 [18].

Due to the wide range of η_{lx} observed in coatings preparation we are going to consider below different scenarios and possible diapason of the latex coating behaviours at certain conditions.

4.1.1. Homogeneous latex layer

For a random packing of monosize spheres the range of $\varepsilon_{lx} = 0.26$–0.4 is the most probable porosity [53,54], which agrees with the latex layer porosity estimations [18,19]. Let us, for application Eq. (8), represent the tortuosity factor in the form [1,55–58]:

$$\tau = T^2 \tag{11}$$

where $T = L'/L$ is the tortuosity, defined as a ratio of diffusion pathway length L' to the porous medium thickness L [55,56,59–62].

Assuming the tortuosity as a functional dependence of the form $T \sim 1/\varepsilon_{lx}^{1/2}$ [50,51,63] then from Eqs. (8) and (11) we have $\eta_{lx} = \varepsilon_{lx}^2 = 0.068$–$0.16$ that is higher than measured upper limit of $\eta_{lx} \sim 0.04$ [18]. Hence, the microstructure simulated by monosize sphere pacing gives a highly permeable coating but effects accompanying the formation process of biocatalytic coating are reduce the permeability. One of the reasons of η_{lx} lowering is latex particles coalescence. Latex film, produced without coalescence control, gives values for relative diffusion conductivity around 3×10^{-5} [18] that well fits with the void fraction network after latex film formation estimated to be less than 0.6% [64]: using mentioned above model we obtain $\eta_{lx} = \eta_f = \varepsilon_{lx}^2 = 3.6 \times 10^{-5}$, where η_f is a polymer film relative diffusion conductivity.

4.1.2. Latex coatings with partial polymer particles coalescence

Latex films produced with the application of a mixture of latex with carbohydrate (sucrose or trehalose), depending on the additive amount, give values for relative diffusion conductivity up to 0.048 (0.6 vol carbohydrate/vol dry polymer) [18,65] that corresponds to porosity around $\varepsilon_{lx} = 0.22$.

Based on obtained estimation, it is possible concluded that the formula $\eta_{lx} = \varepsilon_{lx}^2$ applicable for simulation of homogenous latex layer with different degree particles coalescence: from monodispersed sphere packing up to dense films with pore network.

Another effect that reduces the latex coating permeability is the latex particle flattening on the support surface used for the layer formation.

4.1.3. Latex layer with flattened polymer particle skin

Cryogenic SEM micrograph shows that flattening affects the layer 0.3 μm thick and the extrapolation of experimental data up to 0.3 μm layer gives for relative diffusion conductivity of flattened layer (skin) a value of 3×10^{-4} for the latex containing 0.1 vol glycerol/vol dry polymer [18]. The skin resistance is defined by two factors.

First, it is a mechanical reducing in free cross-section area accessible for diffusion. The skin of thickness of one particle size has the tortuosity $T \approx 1.0$ and hence this part of the skin relative diffusion conductivity would be defined by free cross-section fraction $\varepsilon_s \approx 0.1$ (variation in the value is available due to degree of flattening effect).

The second factor is a migration of a stabiliser in the porous latex layer to the support surface (layer bottom – flattened skin) during the layer formation. The migration for porous layer with arrested coalescence acts contrary to a conventional stabiliser migration during the film formation to the surface of the latex film [66–69]. Finally, in the end of drying procedure a stabiliser

can form the film covering part of pores (clusters) in the skin layer [67,70].

Because the cluster nature of the film distribution in the skin pores, parameter η_{sp}, Eq. (10), becomes complex and dependent on the fraction of pores occupied by film, φ:

$$\eta_{sp} = \frac{1}{[\varphi/\eta_f + (1-\varphi)/\eta_s]} \quad (12)$$

and Eq. (9) becomes

$$\eta_{(lx+s)} = \frac{1}{\{y_{lx}/\eta_{lx} + (1-y_{lx})/[1/(\varphi/\eta_f + (1-\varphi)/\eta_s)]\}} \quad (13)$$

where, in the case of [18], by assuming $\eta_f = 3\times10^{-5}$ and $\eta_s = \varepsilon_s = 0.1$, for measured the skin layer $\eta_{sp} = 3\times10^{-4}$, the fraction of pores occupied by the film is $\varphi = 0.1$.

Model of the coating with skin (9) is simulated for conditions defined by relation (10) and (13) and shown in Fig. 2.

The following scenarios are shown in Fig. 2. Curves 1, 1′–3, 3′ is the model (13): coating with skin of flattened particles partially occupied by film: $\eta_f = 3\times10^{-5}$, $\eta_s = \varepsilon_s = 0.1$. Curves 4 and 5 are the model (9) and (10) of the coating with skin and nano-particles distributed in the skin pore. Other parameters are presented in Table 1. Data set A correspond to $\eta_{(lx+s)}$ measured by [18] which refer to the latex film containing 0.1 vol glycerol/vol dry polymer. Data set B is the results obtained in actual measurements for different concentration of sucrose per kg of

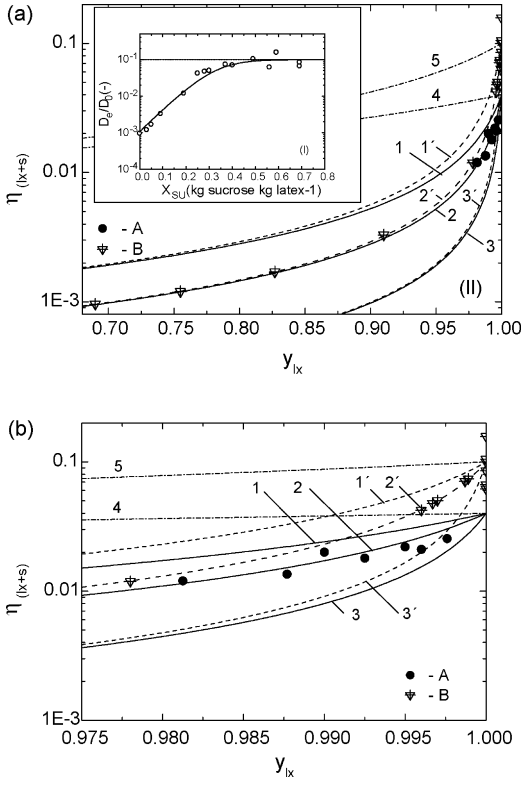

Fig. 2. Dependence of the coating layer with flattened skin $\eta_{(lx+s)}$ on the latex layer thickness fraction y_{lx} at different conditions. Curves 1, 1′–3, 3′ is the model (13) and 4–5 is a model (9) with (10). A, data [18]; B, actual measurements. In Fig. 2b the region of $y_{lx} > 0.975$ is shown in larger scale. Model parameters and comments see in the text.

Table 1
Parameters used for simulation of coating with skin in Fig. 2

Curve number	Latex layer porosity, ε_{lx}	Fraction of pores occupied by the film, φ	Nano-particles in pores of skin, ε_p
1	0.20	0.05	–
2		0.10	–
3		0.30	–
1′	0.32	0.05	–
2′		0.10	–
3′		0.30	–
4	0.20	–	0.26
5	0.32	–	

the latex, Fig. 2a, window (I). For data B was used a condition $\varepsilon_{lx} = 0.32$.

The obtained model values (Fig. 2) show that the skin layer with pores partially filled by polymer film formed from the latex stabiliser significantly affect the skin permeability where as the particle flattening effect himself retards diffusion in order of magnitude less even with accounting formation in the skin pore of dense nano-particles packing with porosity 0.26.

4.2. Composite layer

Composite layer model (6) can be considered as a packing of latex and cell particles but needs to be adapted to the *E. coli* cells.

Rod-like cells of *E. coli* have a ratio δ of a length/diameter around 2:1. The structure of cells packing, depending on cell load, varies from random rod packing up to the dense packing of parallel rods. Using data for a random packing of monosized cylinders [71] we obtain a linear correlation function of packing porosity ε_c versus δ: $\varepsilon_c = 0.3053 + 0.02557\delta$ with a correlation coefficient of 0.9968. From that correlation function for $\delta = 2.0$ the random cell packing porosity is equal $\varepsilon_c = 0.356$. Dixon [72] gives a porosity of 0.36; in the work [73] experimental porosity was 0.33 and for computer simulation, dense packing has the porosity 0.326 and loose has 0.44. From the work, [74] dense and loose packing porosity estimation are 0.325 and 0.41, respectively. From presented data for *E. coli*, porosity $\varepsilon_c = 0.356$ was chosen as the average value. According to [47], for $\delta = 2$ the tortuosity relation has the form $T_c = 1/\varepsilon_c^{0.338}$.

Cell to latex particle volume ratio estimation was made using a formula for the equivalent sphere diameter of cylindrical particles [74,75]: $d_v = 1.145h\delta^{1/3}$, where h is the diameter of the rods, hence for $\delta = 2$ $d_v = 1.4426h$ and for a cell of diameter $h = 1$ μm, $d_v = 1.4426$ μm. This gives the volume ratio of cell/latex particles around 5 and the ratio cell length to latex particle size of about 10.

4.2.1. Analysis of η_{clx} versus cell loading

Experimental data of η_{clx} versus viable cells loading shown in Fig. 8 of the work from [18] reveal deviation from the diffusion models (14) used in [18]:

$$\eta_{clx} = \eta_{lx}\frac{2(1-\phi_c)}{(2+\phi_c)} \quad (14)$$

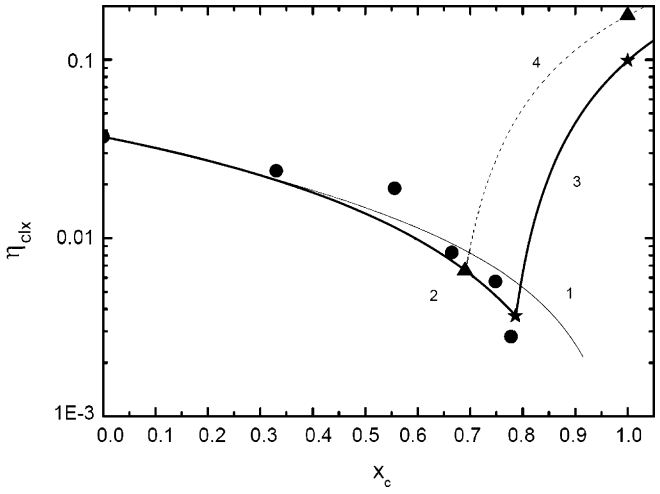

Fig. 3. Dependence of the composite layer η_{clx} on the cell volume fraction x_c in the composite. 1, Eq. (14), 2 and 3, linear model (15) with Eqs. (16) and (17) at $\varepsilon_c^0 = 0.251$. 4, the same model (15) at $\varepsilon_c^0 = 0.356$. Solid circles – data of [18]; stars are minimum porosity points.

Let us consider the composite layer as a binary particulate mixture where the volume fraction of cells, x_c is defined as the ratio of cells volume to the total volume of solid phase (cells + latex particle volumes), hence, $x_c = 0$ at pure latex layer and equal 1.0 at pure cell packing. Data in [18] with cell loading converted to cell volume fraction x_c are shown in Fig. 3, where for pure latex layer ($x_c = 0$) $\eta_{clx} = \eta_{lx} = 0.037$ as it was defined by reference [18]. Above was shown that for the latex packing the relation $\eta_{lx} = \varepsilon_{lx}^2$ is applicable, hence, $\eta_{lx} = 0.037$ corresponds $\varepsilon_{lx} = 0.1924$.

As seen on Fig. 3, Eq. (14) deviates from experimental data (circles) at the region of high *E. coli* cell loading.

Based on the fractional porosity and tortuosity approach [50,51] the relative diffusion conductivity of the composite layer (6) can be written as a function of the cell volume fraction, x_c:

$$\eta_{clx} = \eta_c(x_c)\eta_{lx}(x_c) = [\varepsilon_c(x_c)]^{1.676}[\varepsilon_{lx}(x_c)]^2 \tag{15}$$

where $\eta_c(x_c) = [\varepsilon_c(x_c)]^{1.676}$ is a complex function of the cell packing porosity $\varepsilon_c(x_c)$ and the tortuosity factor $\tau_c = T_c^2$ at $T_c = 1/[\varepsilon_c(x_c)]^{0.338}$.

Since the latex fraction packing structure is mainly defined by the coalescence effect rather than by the cells presence, a linear packing model was chosen [76] to fit the experimental data. According to the model, for mixtures enriched with small (latex) particles the composite porosity depends on the cell content $\varepsilon = \varepsilon_c \cdot \varepsilon_{lx}^0$, whereas for mixtures enriched coarse (*E. coli* cell) particles $\varepsilon = \varepsilon_c^0 \cdot \varepsilon_{lx}$, where ε_{lx}^0 and ε_c^0 are, respectively, porosity of pure latex and cell packing. In the point of minimum porosity $\varepsilon_{min} = \varepsilon_c^0\varepsilon_{lx}^0$ corresponding to the cell volume fraction $x_{c(min)} = (1 - \varepsilon_c^0)/(1 - \varepsilon_c^0 \times \varepsilon_{lx}^0)$ the intersection of both ε functions takes place.

Fractional porosities $\varepsilon_c(x_c)$ and $\varepsilon_{lx}(x_c)$ are as the following

$$\varepsilon_c = \frac{(1 - x_c)}{(1 - x_c\varepsilon_{lx}^0)} \tag{16}$$

$$\varepsilon_{lx} = \frac{(\varepsilon_c^0 + x_c - 1)}{(\varepsilon_c^0 x_c)} \tag{17}$$

where $\varepsilon_{lx}^0 = 0.1924$. For ε_c^0 two values were tested: 0.356 and 0.251 (dense packing).

When the cell loading overcomes the point of minimum porosity, the cell packing changes from random to the dense cell arrangement with $\varepsilon_c^0 = 0.251$, Fig. 3, curve 2 + 3. For comparison Eq. (17), curve 4, for $\varepsilon_c^0 = 0.356$ is shown. Simulation indicates that model curve 2 + 3 gives acceptable approximation composite layer permeability.

Cryo-S.E.M. images of the composite *E. coli* + latex, when the cells were removed, revealed that the latex overlapping occurs close to the cells surface [18]. Perhaps this effect reaches a maximum in the region close to the minimum mixture porosity that explains lower experimental point position at $x_{c(min)}$ than predicted $\eta_{min} = 0.00365$, $x_{c(min)} = 0.787$ marked by solid star. It was previously observed that at the high cell concentration the latex particles could not form a continuous network around the cells and fixed them.

4.3. Three-layer system

The model of three-layer system (5) without latex flattening (skin) effect, $\eta_{(lx+clx)}$, is given by Eq. (18), in the assumption that $\eta_{(lx)1} = \eta_{(lx)2} = \eta_{lx}$

$$\eta_{(lx+clx)} = \frac{1}{((1 - y_{clx})/\eta_{lx} + y_{clx}/\eta_{clx})} \tag{18}$$

where $1 - y_{clx}$ is the summarised thickness fraction of both bottom and top latex layers in the system.

In turn if the skin (first latex particles flattening) effect is taken into account the model may be expressed by Eq. (5) with the following conditions.

The skin layer has characteristics similar to obtained in [18]: $\eta_s = 0.00003$, the skin thickness is equal one latex particle size ~0.3 μm and locates on outer surface one of the latex coatings. Latex coatings have equal relative diffusion conductivity $\eta_{(lx)1} = \eta_{(lx)2} = \eta_{lx}$. Estimated thickness fraction of the skin layer is calculated for the latex coatings thickness of 30 μm each and composite layer thickness 40 μm and is equal to $y_s = 0.003$. Finally, three-layer model becomes

$$\eta_{(lx+clx+s)} = \frac{1}{(y_{lx}/\eta_{lx} + y_{clx}/\eta_{clx} + y_s/\eta_s)} \tag{19}$$

where $y_{lx} = 1 - y_{clx} - y_s$ is the summarised fractional thickness of top and bottom latex coatings and $y_s = 0.003$.

Modelling result for the layered structure with and without the flattened layer (skin) is shown in Fig. 4: the system without skin $\eta_{(lx+clx)}$, curves 1, 1′ and 2, 2′ and with skin $\eta_{(lx+clx+s)}$, curves 1″, 1‴ and 2″, 2‴. All curves marked by 1 are obtained for the minimum packing porosity of the composite layer $\eta_{clx} = 0.00365$ (point marked by solid star in Fig. 3) and curves marked by 2 are built for moderate cell loading $\eta_{clx} = 0.0097$, $x_c = 0.6$. The value of η_{lx} assumed to equal of the composite layer latex matrix in absence of the cells $\eta_{lx} = 0.037$ ($\varepsilon_{lx} = 0.1924$), curves 1, 2 and

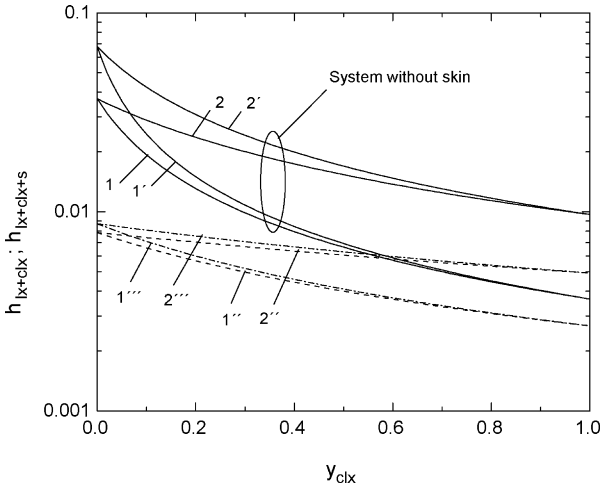

Fig. 4. Dependence of the three-layer system relative diffusion conductivity on fraction thickness of the composite layer y_{clx}. The system without skin $\eta_{(lx+clx)}$, curves 1, 1′ and 2, 2′. The system with skin $\eta_{(lx+clx+s)}$, curves 1″, 1‴ and 2″, 2‴.

1″, 2″, whereas $\eta_{lx} = 0.0676$ ($\varepsilon_{lx} = 0.26$) was used for curves 1′, 2′ and 1‴, 2‴.

The simulation shows that the layered system significantly affected of the cell density packing in composite layer, for instance, curves 1, 2. Previous observations show that the cell loading has critical value when further increasing cell loading does not satisfy the condition of continuous latex network around the cells [18,23]. Estimation provided by [18] gives a critical value around $x_c = 0.7$. For coatings of latex + pigment (latex/pigment size ratio 1:3) the critical pigment volume fraction is determined to be $x_c = 0.6$ [77]. Therefore, cell volume fraction in composite, $x_c = 0.6$, simulates condition below critical loading whereas $x_{c(min)} = 0.787$ gives the system η above the critical cell loading.

Layered system is sensitive to the latex coatings porosity when the composite layer occupies 50% and less of the system thickness (see for example curves 1 and 2) but when the composite layer thickness becomes higher than 40–50% of the overall system thickness the latex coatings effect decline. When the skin effect is introduced into the model, the system permeability is dramatically reduced and, as can be seen in Fig. 4, it becomes the major parameter governing the diffusion. The flattening effect affects a thin layer of the size of one particle and may hardly be the subject of precise control. The composite cell loading is expected to be close to the critical value. Hence only the latex may be considered for optimisation of the layered system permeation.

5. Conclusion

Modelling of porous layered systems containing living cells and partially coalesced latex polymer particles showed that compaction, coalescence, overlapping, and flattening of latex particles appear to be important not only in the process of latex layer formation but also in processes where there is a cell-containing layer. In both cases the overlapping and especially the particles flattening may create skin-like micro-layers that significantly affect the system relative diffusion conductivity. The cell loading in composite layer also affects the overall relative diffusion conductivity.

The layered system is sensitive to the latex coatings porosity when the composite layer occupies 50% and less of the system thickness.

Presence in the system of the skin effect dramatically reduces the system permeability and becomes a major parameter governing the diffusion. It seems that the flattening effect in a thin border layer of the size of one particle and cannot be subject of precise control as well as the composite cell loading that expecting to be close to the critical value.

The latex coating and matrix is a matter for optimisation of the layered system permeation. If the control of polymer particle coalescence and layers (coating/composite layer) thickness is simultaneously achieved, multi-layer systems presenting a wide range of relative diffusion conductivities may be built for different types of living cells for a wide variety of practical applications. The diffusivity of latex layer can be predicted by the simple relation $\eta_{lx} = \varepsilon_{lx}^2$. The composite layer packing follows the linear model of binary particulate packing.

Acknowledgements

The authors wish to thank Fundação para a Ciência e Tecnologia – FCT – for the grant accorded to Dr. Yelshin and for the project POCTI/37500/EQU/2001 that provided the means for the present research. This project had also the contribution of FEDER.

References

[1] J. Bear, Dynamics of Fluids in Porous Media, Dover Publ., Inc, New York, 1972.
[2] R. Aris, The Mathematical Theory of Diffusion and Reaction in Permeable Catalysts, vol. 1, Clarendon Press, Oxford, 1975.
[3] T.K. Sherwood, R.L. Pigford, C.R. Wilke, Mass Transfer, McGraw-Hill, Tokyo, Japan, 1975.
[4] M.B. Moranville, D.P. Kessler, R.A. Greenkorn, Dispersion in layered porous media, AIChE J. 23 (1977) 786–794.
[5] P.A. Tyvand, Approximate formulae for the dispersion coefficients of layered porous media, AIChE J. 26 (1980) 513–517.
[6] R. Rautenbach, R. Albrecht, Membrane Processes, Wiley, UK, 1989.
[7] W.S.W. Ho, K.K. Sirkar, Membrane Handbook, WNR, New York, 1992.
[8] R. Anselmann, Nanoparticles and nanolayers in commercial applications, J. Nanoparti. Res. 3 (2001) 329–336.
[9] E.M. Sparrow, G.S. Beavers, L. Goldstein, P. Bahrami, Flow through permeable beds consisting of layers of different size spheres, AIChE J. 22 (1976) 194–196.
[10] K. Cooksey, K.S. Marsh, L.H. Doar, Predicting permeability and transmission rate for multilayer materials, Food Technol. 53 (1999) 60–63.
[11] C. Chan, M. Lehmann, K. Chan, P. Chan, C. Chan, B. Gruendig, G. Kunze, R. Renneberg, Designing an amperometric thick-film microbial BOD sensor, Biosens. Bioelectron. 15 (2000) 343–353.
[12] S.F. D'Souza, Microbial biosensors, Biosens. Bioelectron. 16 (2001) 337–353.
[13] P. Mulchandani, W. Chen, A. Mulchandani, J. Wang, L. Chen, Amperometric microbial biosensor for direct determination of organophosphate pesticides using recombinant microorganism with surface expressed organophosphorus hydrolase, Biosens. Bioelectron. 16 (2001) 433–437.

[14] R.S. Dubey, S.N. Upadhyay, Microbial monitoring by an amperometric microbial biosensor developed using whole *Pseudomonas* sp., Biosens. Bioelectron. 16 (2001) 995–1000.
[15] M.L. Simpson, G.S. Saylor, B.M. Applegate, S. Ripp, D.E. Nivens, M.J. Paulus, E. Jellison, Bioluminescent-bioreporter integrated circuits form novel whole-cell biosensors, Trends Biotechnol. 16 (1998) 332–338.
[16] M.L. Simpson, G.S. Saylor, J.T. Fleming, B. Applegate, Whole-cell biocomputing, Trends Biotechnol. 19 (2001) 317–323.
[17] I. Willner, B. Willner, Biomaterials integrated with electronic elements: an route to bioelectronics, Trends Biotechnol. 19 (2002) 222–230.
[18] O.K. Lyngberg, C.P. Ng, V. Thiagarajan, L.E. Scriven, M.C. Flickinger, Engineering the microstructure and permeability of thin multilayer latex biocatalytic coatings containing *E. coli*, Biotechnol. Prog. 17 (2001) 1169–1179.
[19] S. Jons, P. Ries, C.J. McDonald, Porous latex composite membranes: fabrication and properties, J. Membr. Sci. 155 (1999) 79–99.
[20] S. Kirsch, A. Pfau, E. Hädicke, J. Leuninger, Interface and bulk properties in films of phase separated dispersion particles, Prog. Org. Coat. 45 (2002) 193–204.
[21] O.K. Lyngberg, V. Thiagarajan, D.J. Stemke, J.L. Schottel, L.E. Scriven, M.C. Flickinger, A patch coating method for preparing biocatalytic films of *Escherichia coli*, Biotechnol. Bioeng. 62 (1999) 44–55.
[22] Z. Huang, V.S. Thiagarajan, O.K. Lyngberg, L.E. Scriven, M.C. Flickinger, Microstructure evolution in polymer latex coatings for whole-cell biocatalyst application, J. Colloid Interface Sci. 215 (1999) 226–243.
[23] V.S. Thiagarajan, Z. Huang, L.E. Scriven, J.L. Schottel, M.C. Flickinger, Microstructure of a biocatalytic latex coating containing viable *Escherichia coli* cells, J. Colloid Interface Sci. 215 (1999) 244–257.
[24] K.L. Swope, M.C. Flickinger, The use of confocal scanning laser microscopy and other tools to characterize *Escherichia coli* in a high-cell-density synthetic biofilm, Biotechnol. Bioeng. 52 (1996) 340–356.
[25] R. Prasad, K.K. Sirkar, Solvent extraction with microporous hydrophilic and composite membranes, AIChE J. 33 (1987) 1057–1066.
[26] U. Beuscher, C.H. Gooding, Characterization of the porous support layer of composite gas permeation membranes, J. Membr. Sci. 132 (1997) 213–227.
[27] J.E. Bailey, D.F. Ollis, Biochemical Engineering Fundamentals, McGraw-Hill, Singapore, 1986.
[28] W.C. Maskell, Tortuosity factor in non-homogeneous membranes, Ber. Bunsen-Ges. Phys. Chem. 97 (1993) 680–683.
[29] S.K. Karode, S.S. Kulkarni, Analysis of transport through thin film composite membranes using an improved Wheatstone bridge resistance model, J. Membr. Sci. 127 (1997) 131–140.
[30] U. Beuscher, C.H. Gooding, The permeation of binary gas mixtures through support structures of composite membranes, J. Membr. Sci. 150 (1998) 57–73.
[31] T.-Q. Li, M. Häggkvist, L. Ödberg, The porous structure of paper coatings studied by water diffusion measurements, Colloids Surf. A: Physicochem. Eng. Aspects 159 (1999) 57–63.
[32] U. Beuscher, C.H. Gooding, The influence of the pore support layer of composite membranes on the separation of binary gas mixtures, J. Membr. Sci. 152 (1999) 99–116.
[33] R. Cachon, P. Molin, C. Diviès, Modelling of continuous pH-stat stirred tank reactor with Lactococcus lactis ssp. lactis bv. diacetylactis immobilized in calcium alginate gel beads, Biotechnol. Bioeng. 47 (1995) 567–574.
[34] R. Scharer, Md.M. Hossain, D.D. Do, Determination of total and active immobilized enzyme distribution in porous solid supports, Biotechnol. Bioeng. 39 (1992) 679–687.
[35] H. Fukuda, H. Morikawa, Secretive fermentation of g—linolenic acid production using cells immobilised in biomass support particles, in: G.W. Moody, P.B. Baker (Eds.), Bioreactors and Biotransformations, Elsevier, London, UK, 1987, pp. 386–394.
[36] Y. Fukushima, K. Okamura, K. Imai, H. Motai, A new immobilization technique of whole cells and enzymes with colloidal silica and alginate, Biotechnol. Bioeng. 32 (1988) 584–594.
[37] C.D. De Gooijer, R.H. Wijffels, J. Tramper, Growth and substrate consumption of Nitrobacter agilis cells immobilized in carrageenan: Part 1. Dynamic modelling, Biotechnol. Bioeng. 38 (1991) 224–231.
[38] J.P. Arnaud, C. Lacroix, Diffusion of lactose in k-carrageenan/locust bean gum gel beads with or without entrapped growing lactic acid bacteria, Biotechnol. Bioeng. 38 (1991) 1041–1049.
[39] H. Fukuda, Immobilized macroorganism bioreactors, in: J.A. Asenjo, J.C. Merchuk (Eds.), Bioreactors System Design, M.Dekker, New York, 1995, p. 350.
[40] H.H.P. Fang, Microbial distribution and syntrophic association in UASB granules, in: Proceedings of 8th International Conf. on Anaerobic Digestion, vol. 1, May 25–29, 1997, Sendai, Japan, 1997, pp. 83–90.
[41] P. Gikas, A.G. Livingston, Specific ATP and specific oxygen uptake rate in immobilized cell aggregates: experimental results and theoretical analysis using a structured model of immobilized cell growth, Biotechnol. Bioeng. 55 (1997) 660–673.
[42] F. Leonhardt, P. Hortschansky, J. Drechsler, H.D. Pohl, Separation of recombinant *E. coli* culture broths by adsorption to modified carriers and controlled release of an expressed protein, Bioprocess Eng. 17 (1997) 23–29.
[43] E.J.T.M. Leenen, A.A. Boogert, A.A.M. Van Lammeren, J. Tramper, R.H. Wijffels, Dynamics of artificially immobilized *Nitrosomonas europaea*: effect of biomass decay, Biotechnol. Bioeng. 55 (1997) 630–641.
[44] C. Picioreanu, M.C.M. Loosdrecht van, J.J. Heijnen, A new combined differential-discrete cellular automaton approach for biofilm modeling: Application for growth in gel beads, Biotechnol. Bioeng. 57 (1998) 718–731.
[45] B.A. Westrin, A. Axelsson, Diffusion in gels containing immobilized cells: A critical review, Biotechnol. Bioeng. 38 (1991) 439–446.
[46] M. Mota, J.A. Teixeira, A. Yelshin, Immobilized particles in gel matrix-type porous media. Homogeneous porous media model, Biotechnol. Prog. 17 (2001) 860–865.
[47] M. Mota, J.A. Teixeira, A. Yelshin, Immobilized particles in gel matrix-type porous media. Non-homogeneous cell distribution, Biotechnol. Prog. 18 (2002) 807–814.
[48] M. Mota, J.A. Teixeira, A. Yelshin, Tortuosity in bioseparations and its application to food processes, in: E. Feyo de Azevedo, K. Ferreira, P. Luben, Osseweijer (Eds.), Proceedings of 2nd European Symposium on Biochemical Engineering Science, Porto, 16–19 Sept. 1998, Univ. of Porto, Porto, Portugal, 1998, pp. 93–98.
[49] M. Mota, J.A. Teixeira, A. Yelshin, Image analysis of packed beds of spherical particles of different sizes, Sep. Purific. Technol. 15 (1999) 59–68.
[50] M. Mota, J.A. Teixeira, R. Bowen, A. Yelshin, Effect of tortuosity on transport properties of mixed granular beds, in: Proceedings of 8-th World Filtration Congress, vol. 1, 3–7 April 2000, Filtration Society, Brighton, UK, 2000, pp. 57–60.
[51] M. Mota, J.A. Teixeira, A. Yelshin, Binary spherical particle mixed beds porosity and permeability relationship measurement, Trans. Filtr. Soc. 1 (2001) 101–106.
[52] Y. Shimizu, K.-I. Shimodera, A. Watanabe, Cross-flow microfiltration of bacterial cells, J. Ferm. Bioeng. 76 (1993) 493–500.
[53] M. Shahinpoor, Statistical mechanical considerations on the random packing of granular materials, Powder Technol. 25 (1980) 163–176.
[54] M. Suzuki, K. Makino, M. Yamada, K. Iinoya, A study on the coordination number in a system of randomly packed, uniform-sized spherical particles, Int. Chem. Eng. 21 (1981) 482–488.
[55] J.C. Giddings, Dynamics of Chromatography. Part I. Principles and Theory, M. Dekker, New York, 1965.
[56] E.L. Cussler, Diffusion: Mass Transfer in Fluid Systems, Cambridge Univ. Press, Cambridge, 1984.
[57] M. Suzuki, Adsorption Engineering, Kodansha-Elsevier, Tokyo, 1990.
[58] K. Miyabe, M. Suzuki, Chromatography of liquid-phase adsorption on octadecylsilyly-silica gel, AIChE J. 38 (1992) 901–910.
[59] J.A. Currie, Gaseous diffusion in porous media. Part 2. - Dry granular materials, Br. J. Appl. Phys. 11 (1960) 318–324, August.
[60] C.N. Satterfield, Mass Transfer in Heterogeneous Catalysis, M.I.T. Press, Cambridge, England, 1970.
[61] F.L. Tye, Tortuosity, Chem. Ind. (1982) 322–326.
[62] P.R. Johnston, The most probable pore-size distribution in fluid filter media. II. Determining the size of the average pore from fluid permeability measurements, J. Test. Eval. 11 (1983) 122–125.

[63] M. Mota, J.A. Teixeira, A. Yelshin, Immobilised particles in gel matrix-type porous media. Homogeneous porous media model, in: M. Mota, E. Ferreira (Eds.), IV Iberian Congress on Biotechnology, I Iberio-American Meeting on Biotechnology, BIOTEC-98, 12–15 July, 1998, Book of Abstracts, Barbosa & Xavier, Lda, Braga, Portugal, 1998, p. 211.
[64] J.L. Keddie, Film formation of latex, Mater. Sci. Engin. 21 (1997) 101–170.
[65] P.A. Steward, J. Hearn, M.C. Wilkinson, Studies in permeation through polymer latex films. II. Permeation modification by sucrose addition, Polym. Int. 38 (1995) 13–22.
[66] S. Lam, A.C. Hellgren, M. Sjöberg, K. Holmberg, H.A.S. Schoonbrood, M.J. Unzué, J.M. Asua, K. Tauer, D.C. Sherrington, A.M. Gonu, Surfactants in heterophase polymerization: a study of film formation using atomic force microscopy, J. Appl. Polym. Sci. 66 (1997) 187–198.
[67] A. Tzitzinou, P.M. Jenneson, A.S. Clough, J.L. Keddie, J.R. Lu, P. Zhdan, K.E. Treacher, R. Satguru, Surfactant concentration and morphology at the surfaces of acrylic latex films, Prog. Org. Coat. 35 (1999) 89–99.
[68] F. Belaroui, Y. Grohens, H. Boyer, Y. Holl, Depth profiling of small molecules in dry latex films by confocal Raman spectroscopy, Polymer 41 (2000) 7641–7645.
[69] F. Belaroui, M.P. Hirn, Y. Grohens, P. Marie, Y. Holl, Distribution of water-soluble and surface-active low-molecular-weight species in acrylic latex films, J. Colloid Interface Sci. 261 (2003) 336–348.
[70] E. Teixeira-Neto, G. Kaupp, F. Galembeck, Spatial distribution of serum solutes on dry latex sub-monolayers determined by SEPM, SNOM and SC microscopy, Colloids Surf. A: Physicochem. Eng. Aspects 243 (2004) 79–87.
[71] A.B. Yu, R.P. Zou, N. Standish, Modifying the linear packing model for predicting the porosity of nonspherical particle mixtures, Ind. Eng. Chem. Res. 35 (1996) 3730–3741.
[72] A.G. Dixon, Correlations for wall and particle shape effects on fixed bed bulk voidage, Can. J. Chem. Eng. 66 (1988) 705–708.
[73] G.T. Nolan, P.E. Kavanagh, Random packing of nonspherical particles, Powder Technol. 84 (1995) 199–205.
[74] R.P. Zou, A.B. Yu, Porosity calculation of mixtures of fibrous particles, China Particuology 1 (2003) 27–32.
[75] A.B. Yu, N. Standish, A. McLean, Porosity calculation of binary mixtures of non-spherical particles, J. Am. Ceram. Soc. 76 (1993) 2813–2816.
[76] M. Mota, J.A. Teixeira, A. Yelshin, W.R. Bowen, Interfering of coarse particles with finest of different shape in cake model, Miner. Eng. 16 (2003) 135–144.
[77] D.I. Lee, The structure of model coatings: latex-bound plastic pigment coatings, Prog. Org. Coat. 45 (2002) 341–358.
[78] M. Fidaleo, S. Charaniya, C. Solheid, U. Diel, M. Laudon, H. Ge, L.E. Scriven, M.C. Flickinger, A model system for increasing the intensity of whole-cell biocatalysis: investigation of the rate of oxidation of d-sorbitol to l-sorbose by thin bi-layer latex coatings of non-growing Gluconobacter oxydans, Biotechnol. Bioeng. 95 (2006) 446–458.
[79] M.C. Flickinger, J.L. Schottel, D.R. Bond, A. Aksan, L.E. Scriven, Painting and printing living bacteria: engineering nanoporous biocatalytic coatings to preserve microbial viability and intensify reactivity, Biotechnol. Prog. 23 (2007) 2–17.
[80] M. Kizilyalli, J. Corish, R. Metselaar, Definitions of terms for diffusion in the solid state (IUPAC Recommendations 1999), Pure Appl. Chem. 71 (1999) 1307–1325.
[81] Diffusivity. http://www.wordwebonline.com/en/DIFFUSIVITY.